# Atom probe tomography of a commercial light emitting diode

**D J Larson[1,*], T J Prosa[1], D Olson[1], W Lefebvre[2], D Lawrence[1], P H Clifton[1] and T F Kelly[1]**

[1] CAMECA Instruments, Inc., 5500 Nobel Drive, Madison, WI 53711 USA
[2] GPM UMR CNRS 6634, Université de Rouen, Saint Etienne du Rouvray 76801 FRANCE

**Summary**: The atomic-scale analysis of a commercial light emitting diode device purchased at retail is demonstrated using a local electrode atom probe. Some of the features are correlated with transmission electron microscopy imaging. Subtle details of the structure that are revealed have potential significance for the design and performance of this device.

## 1. Introduction

Gallium nitride (GaN) has been successfully used as the fundamental material for a wide range of optoelectronic devices [1]. Undoped GaN emits in the ultra-violet (UV), and alloying it with indium or aluminum produces emission with wavelengths ranging from the green to the deep UV. As a result, GaN-based multiple quantum well (MQW) structures are used as the active regions of commercial light-emitting diodes (LEDs) and laser diodes.

Atom probe tomography (APT) provides unique capabilities for nanoelectronic device characterization including three-dimensional compositional mapping of a relevant volume (>$10^6$ $nm^3$), high detection efficiency (>50%), and good sensitivity (<10 ppm) [2]. Although long applied to metals and some semiconductors (see [3] and references contained within), APT has also more recently been applied to semiconducting and insulating materials used in microelectronic devices [4-6]. This change has been enabled by the recent commercial development of laser-pulsed atom probe systems, which were first demonstrated in the 1980s [7]. One application of APT in the microelectronics industry which is less common, however, is competitive analysis and/or failure (FA). In order to facilitate FA of microelectronic structures, a specimen must first be fabricated from a specific, individual device and then satisfactorily survive analysis. As a step on the path toward feasibility for FA using APT, we have collected data from an individual commercial LED originating as a fully packaged device.

## 2. Experimental

OSRAM 455 nm Golden Dragon® Plus LEDs were purchased from a retail supplier, depackaged, and fabricated into APT-compatible specimens using standard focused-ion-beam (FIB) methods [8-10] with a backside preparation direction [11]. Specimen preparation was carried out in an FEI Novalab dual-beam FIB microscope with an Omniprobe AP200 *in-situ* micromanipulator. Scanning transmission electron microscopy observations were performed along the <01-10> orientation of the wurtzite GaN structure with a JEM ARM 200F operating at 200 kV equipped with a Schottky field emission gun. APT data collection was performed on a CAMECA local electrode atom probe (LEAP ®) 4000X HR operated in a 500 kHz pulsed 355 nm laser mode with a pulse energy of 3-70 fJ (adjusted during the run to maintain a

* David.larson@ametek.com

constant charge-state ratio of 0.5 for $Ga^{++}/Ga^{+}$). The specimen base temperature was 25 K and the ion detection rate was 3.0% (three ions detected for every 100 laser pulses).

Figure 1 shows a sequence of images during the specimen preparation process from the initial surface of the wafer after depackaging (Figure 1b) to the final state of FIB annular sharpening [12] of the tip (Figure 1d).

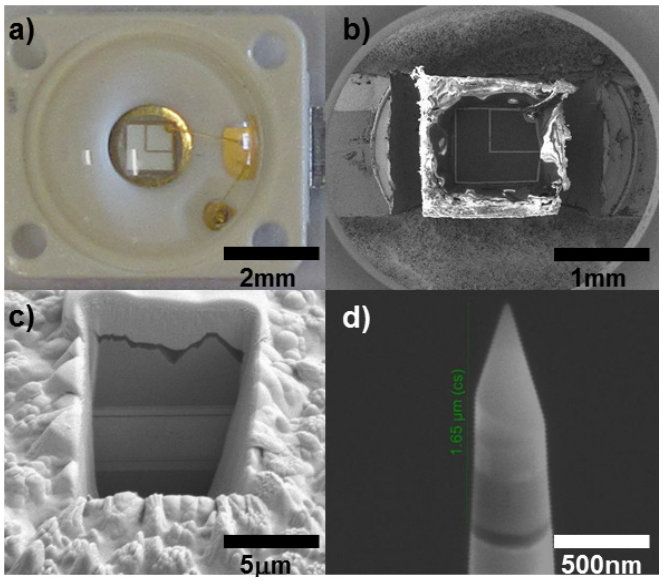


**Figure 1**. Depackaging and FIB preparation of a commercial GaN device for APT analysis: a) initial LED, b) SEM image of depackaged device, c) FIB-milled trenches, d) the final specimen following annular milling.

## 3. Results and Discussion

In order to have as much information as possible regarding details of the LED structure, specimens were also prepared and analyzed in both a CAMECA SXFive electron microprobe and a JEM ARM 200F scanning transmission electron microscope (STEM). In the electron microprobe, signals from Al and In were analyzed in order to determine the location of the In MQW region of interest. In the STEM, a high-angle annular-dark-field image was obtained from a portion of the region of interest and is shown in Figure 2. Five repeats of high image intensity are visible in the image. This microstructure would later be determined by APT as InGaN/GaN quantum wells. From Figure 2, the average width of the bright layers (InGaN) and the dark layers (GaN) is measured to be 3.5±0.2 nm and 4.4±0.2 nm, respectively. This information is used to confirm the spatial reconstruction accuracy for APT data.

Following spectral peak identification in the APT data, a three-dimensional atom map may be created, as shown in Figure 3a. The overall approximate concentration of the APT data is 48.3at.%Ga-50at.%N-0.85at.%In-0.75at.%Al-0.14at.%Mg. Figure 3a shows that the data are highly structured with four distinct regions immediately identifiable: 1) a region of Mg doping (to form p-type GaN) near the left side of the structure, 2) an Al-rich region, 3) a region of In-rich MQWs, and 4) an In-based superlattice structure near the right side of the data.

The Mg distribution is visually non-uniform suggesting that some fraction of the dopant may be electrically inactive [13, 14]. The extent of this non-uniformity may be quantified using standard analysis methods [15] which employ an algorithm using a maximum separation distance ($D_{max}$)

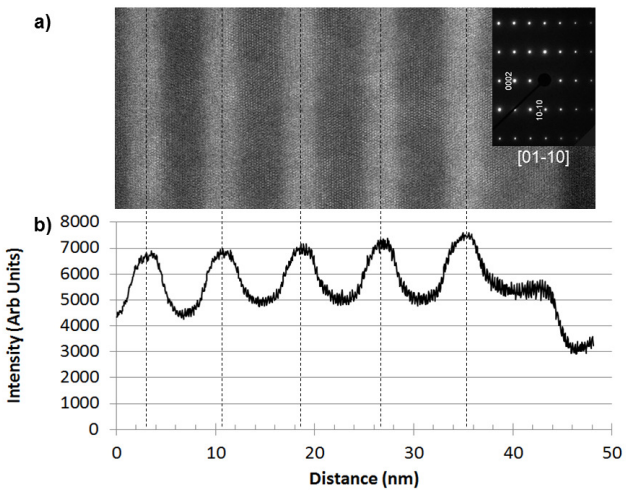


**Figure 2**. (a) High-angle annular-dark-field image of the In MQW region of the OSRAM 455 nm Golden Dragon Plus LED and (b) image intensity profile showing five layers of high intensity. The average distance between the layers (dashed lines) is 7.9 nm.

between atoms. Using a $D_{max}$ value of 1.5 nm produces 69 clusters identified with a mean concentration of Mg of ~10 at.%. The clusters contain an average 21 Mg atoms with a most likely number of atoms per cluster of five to ten atoms. The average cluster volume is ~20 $nm^3$ and the average cluster diameter is ~3 nm.

Adjacent to the region of Mg clusters is a region of high Al concentration (Figure 3). The region is an electron blocking layer (EBL), which improves device performance by preventing carrier migration in the wrong direction (which in this case is electrons moving left to right in Figure 3). The concentration of the EBL, as calculated using an isoconcentration surface enclosing the region of space containing at least 5 at.% Al, is found to be 9.68 at.% Al (estimate of standard error 0.02 at.%). The EBL appears asymmetric, with a higher Al concentration (nearly 15 at.%) on the right edge, as shown in Figure 3b.

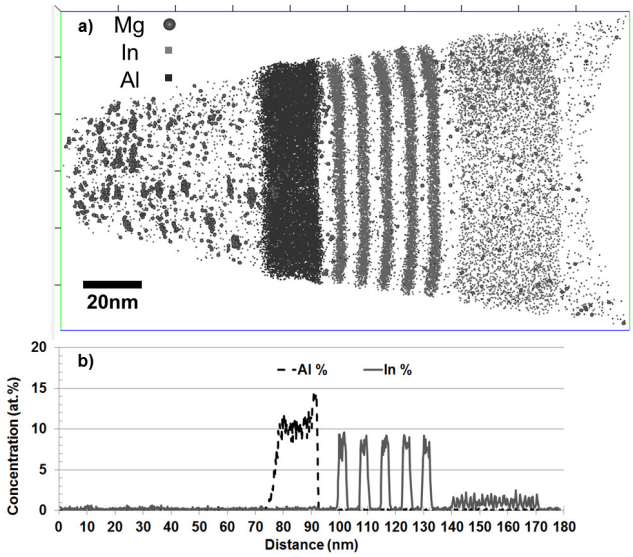


**Figure 3**. (a) APT atom map of the OSRAM 455 nm Golden Dragon Plus LED showing Mg atoms as large spheres, In atoms as small grey dots and Al atoms as small black dots (for clarity, Ga and N atoms are not shown) and (b) concentration profile suggesting four distinct chemical regions within the dataset.

To the right of the EBL in Figure 3 is the region containing In-rich MQWs. As observed in the TEM image in Figure 2, there are five individual wells. The concentration profile in Figure 3b shows that each well reaches approximately 8at.% In. Enclosing and summing the region of space containing at least 3at.% In and calculating a concentration produces 7.3at.% In (note that this is a somewhat arbitrary measurement as it is summed over multiple quantum wells and also depends on the choice of the 3at.%In isoconcentration surface). Qualitatively the wells do not appear to be asymmetric in concentration or in interface intermixing (Figure 3b). This is confirmed by an estimation of the internal interface roughness [16] based on the 3at.% In isoconcentration surface separating each well from the inter-well GaN region. Comparing the distribution of each lower and upper (proceeding right to left in Figure 3) individual interface measurements, we find that the means are not statistically different, with the mean values of RMS roughness being 0.28 nm and 0.24 nm for the lower and upper interfaces, respectively.

On the far right side of Figure 3 there is another region of non-uniform In concentration. Closer investigation of the APT data from this region reveals a superlattice structure of 21 In-rich layers (Figure 4). These layers are spaced ~1.5 nm from each other. When binned in 0.3 nm bins (to minimize statistical variation) the superlattice In concentrations range from 0.5at.% to 1.5at.%.

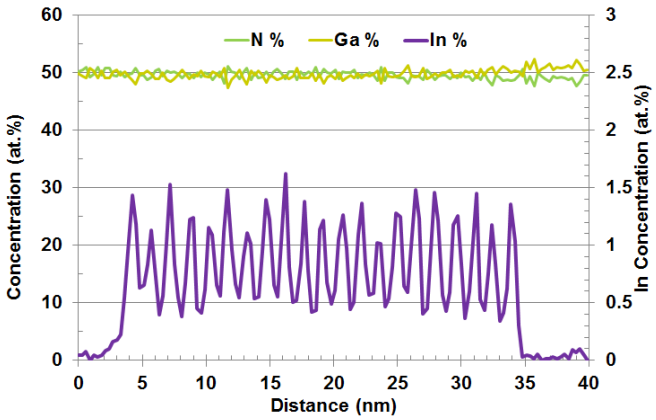


**Figure 4**. Superlattice structure showing 21 layers having a spacing of ~1.5 nm and In concentrations of ~1at.%.

## 4. Conclusion

Many subtle details of the microstructure and composition emerge from

the LEAP analysis of this commercial device. These details provide crucial insights into the design and operation of the device. Many of these features would not be apparent with other techniques especially the Mg clustering and the In superlattice but are readily observed in a single experiment with the LEAP.

**Acknowledgements**

The authors would like to thank our colleagues at CAMECA Instruments, Inc., who assisted in assembling the materials presented in this manuscript, including R. Ulfig, B. Geiser, D. Giddings, S. Strennen, J. Olson, D. Lenz, J. Bunton, J. Shepard, T. Payne, E. Strennen and E. Oltman.

**References**

[1] Schubert E F 2006 *Light Emitting Diodes.* (Cambridge: Cambridge University Press)
[2] Kelly T F and Larson D J 2012 Atom Probe Tomography 2012 *Annual Reviews of Materials Research* **42** 1-31
[3] Miller M K, Cerezo A, Hetherington M G and Smith G D W 1996 *Atom Probe Field Ion Microscopy* (Oxford: Oxford University Press)
[4] Kelly T F, Larson D J, Thompson K, Alvis R L, Bunton J H, Olson J D and Gorman B P 2007 Atom Probe Tomography of Electronic Materials *Annual Review of Materials Research* **37** 681-727
[5] Larson D J, Lawrence D, Lefebvre W, Olson D, Prosa T J, Reinhard D A, Ulfig R M, Clifton P H, Bunton J H, Lenz D, Renaud L, Martin I and Kelly T F 2011 Toward Atom Probe Tomography of Microelectronic Devices *Journal of Physics: Conference Series* **326** 012030
[6] Larson D J, Prosa T J, Lawrence D, Geiser B P, Jones C M and Kelly T F 2011 *Handbook of Instrumentation and Techniques for Semiconductor Nanostructure Characterization,* ed R Haight*, et al.* (London: World Scientific Publishing) 407-77
[7] Kellogg G L and Tsong T T 1980 Pulsed-laser atom-probe field-ion microscopy *Journal of Applied Physics* **51** 1184-94
[8] Larson D J, Foord D T, Petford-Long A K, Cerezo A and Smith G D W 1999 Focused ion-beam specimen preparation for atom probe field-ion microscopy characterization of multilayer film structures *Nanotechnology* **10** 45-50
[9] Miller M K, Russell K F, Thompson K, Alvis R and Larson D J 2007 Review of Atom Probe FIB-Based Specimen Preparation Methods *Microsc. Microanal.* **13** 428-36
[10] Thompson K, Lawrence D J, Larson D J, Olson J D, Kelly T F and Gorman B 2007 In-Situ Site-Specific Specimen Preparation for Atom Probe Tomography *Ultramicroscopy* **107** 131-9
[11] Prosa T J, Lawrence D, Olson D, Larson D J and Marquis E A 2009 Backside Lift-Out Specimen Preparation: Reversing the Analysis Direction in Atom Probe Tomography *Microsc. Microanal.* **15** 298-9
[12] Larson D J, Foord D T, Petford-Long A K, Liew H, Blamire M G, Cerezo A and Smith G D W 1999 Field-Ion Specimen Preparation Using Focused Ion-Beam Milling *Ultramicroscopy* **79** 287-93
[13] Fair R B and Weber G R 1973 Effect of complex formation on diffusion of arsenic in silicon *Journal of Applied Physics* **44** 273-9
[14] Fahey P M, Griffin P B and Plummer J D 1989 Point defects and dopant diffusion in silicon *Reviews of Modern Physics* **61** 289-384
[15] Marquis E A and Hyde J M 2010 Applications of atom-probe tomography to the characterisation of solute behaviour *Materials Science and Engineering R* **69** 37-62
[16] O'Neill R W, Larson D J, Thompson K, Kunicki T C and Geiser B P 2006 Measuring the Roughness of Buried Interfaces in Nanostructures by Local Electrode Atom Probe Analysis *Microsc. Microanal.***12** 1746-8